

Electronic Supporting Information

for

Ln(III)-complexes of a DOTA analogue with an ethylenediamine pendant arm as pH-responsive PARACEST contrast agents

Tereza Krchová^a, Andrea Gálisová^b, Daniel Jiráček^{b,c}, Petr Hermann^a, Jan Kotek^a

^a Department of Inorganic Chemistry, Faculty of Science, Universita Karlova (Charles University), Hlavova 2030, 128 43 Prague 2, Czech Republic. Tel.: +420-221951261. Fax: +420-221951253. E-mail: modrej@natur.cuni.cz.

^b Department of Radiodiagnostic and Interventional Radiology, Magnetic Resonance Unit, Institute for Clinical and Experimental Medicine, Vídeňská 1958/9, Prague 4, 140 21 Czech Republic.

^c Institute of Biophysics and Informatics, 1st Faculty of Medicine, Universita Karlova (Charles University), Salmovská 1, 120 00 Prague 2, Czech Republic.

Contents

X-Ray diffraction.....	2
Temperature dependence of ¹ H NMR spectra of [Eu(do3aNN)] in D ₂ O.....	3
Temperature dependence of ¹ H NMR spectra of [Yb(do3aNN)] in D ₂ O.....	4
pH dependence of ¹ H NMR spectra of [Yb(do3aNN)].....	5
Low-temperature ¹ H NMR spectra of [Eu(do3aNN)] and [Yb(do3aNN)] in H ₂ O.....	6
Temperature dependence of NMR spectra of [Eu(H _n do3aNN)] in H ₂ O.....	7
Dependence of Z-spectra of [Eu(H _n do3aNN)] and [Yb(H _n do3aNN)] on presaturation intensity.....	8
Tentative visualization of TSA isomers differing in chirality of coordinated secondary amino group.	10
pH dependence of MTR of [Eu(H _n do3aNN)] complex.....	11
¹ H and ¹³ C{ ¹ H} NMR spectra of H ₃ do3aNN.....	12
Potentiometric studies – protonation and stability constants of H ₃ do3aNN and its Eu(III)/Yb(III) complexes.....	13
Schemes – suggested protonation sites of complex species.....	16
UV-Vis spectrophotometry.....	17
References.....	18

X-Ray diffraction

The single-crystal of **6**·2H₂O was prepared from concentrated aqueous solution of the compound **6** by a slow diffusion of EtOH vapours. The diffraction data were collected employing ApexII CCD diffractometer using Mo-*K*_α radiation ($I = 0.71073 \text{ \AA}$) at 150(1) K and analysed using the SAINT V8.27B (Bruker AXS Inc., 2012) program package. The structures were solved by direct methods (SHELXS97¹) and refined by full-matrix least-squares techniques (SHELXL97²). All non-hydrogen atoms were refined anisotropically. Carbon atoms of the ethylene group of amine pendant arm were found to be disordered in two positions with relative occupancy 56:44. Hydrogen atoms attached to carbon atoms were fixed in theoretical positions using a riding model with $U_{\text{eq}}(\text{H}) = 1.2 U_{\text{eq}}(\text{C})$, and those belonging to the oxygen or nitrogen atoms were fully refined.

Crystal data

6·2H₂O: C₁₉H₃₈N₆O₉, $M = 494.55$, monoclinic, $a = 7.7686(3)$, $b = 15.4411(5)$, $c = 19.4703(7) \text{ \AA}$, $b = 93.165(2)^\circ$, $U = 2332.01(14) \text{ \AA}^3$, space group $P2_1/c$, $Z = 4$, 4582 total reflections, 3599 intense reflections, $R_1[I > 2\sigma(I)] = 0.0596$, $wR_2(\text{all data}) = 0.1757$. CCDC-1430249.

The found protonation scheme (Figure S1) is similar to those found previously for related 2-aminoethyl analogues³ – two protons are bound to the mutually *trans* macrocycle amino groups bearing acetate moieties and the third one belongs to the “odd” acetate moiety. The conformation of the macrocyclic unit is (3,3,3,3)-B, as usually observed for the double-protonated cyclen rings.⁴ Such a conformation is stabilized by the intramolecular hydrogen bonds between the protonated and non-protonated macrocycle amino groups. The whole crystal structure is stabilized by the extended hydrogen bonds network between ligand and the water solvate molecules.

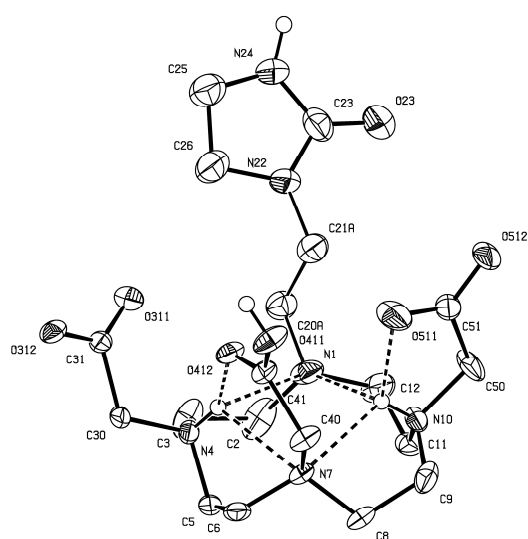
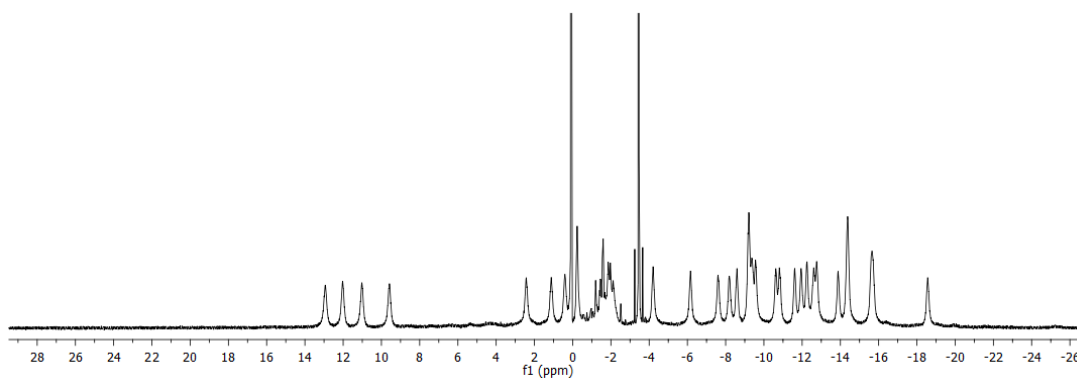


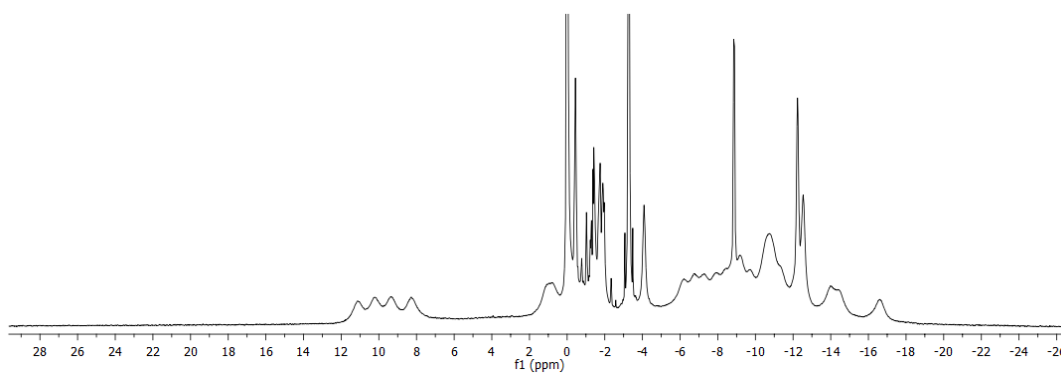
Figure S1 Molecular structure of **6** found in the crystal structure of **6**·2H₂O. Carbon-bound hydrogen atoms are omitted for clarity reasons. Hydrogen bonds are dashed.

Temperature dependence of ^1H NMR spectra of $[\text{Eu}(\text{do3aNN})]$ in D_2O

25 °C



50 °C



75 °C

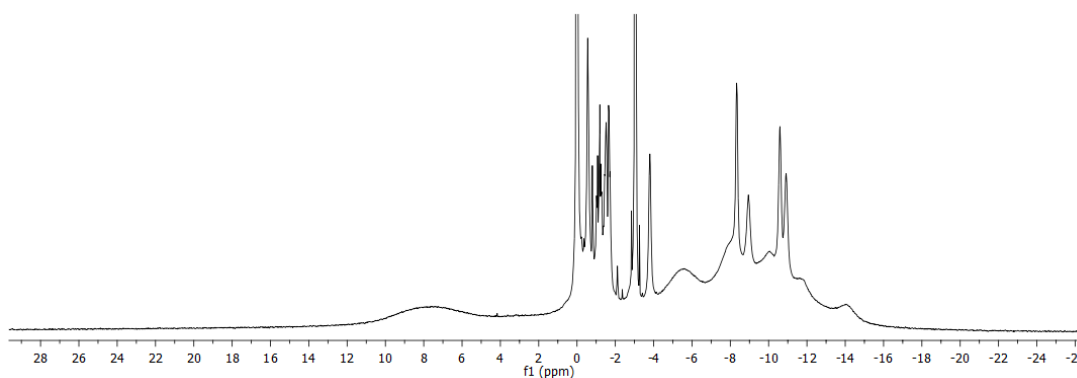
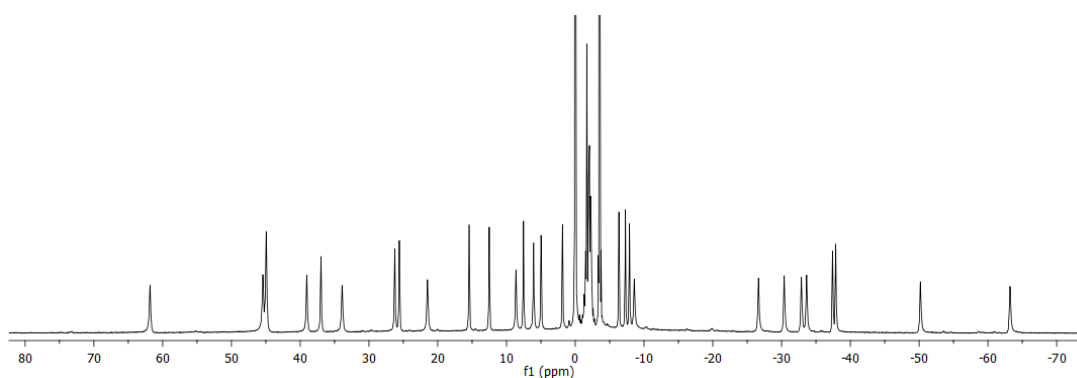


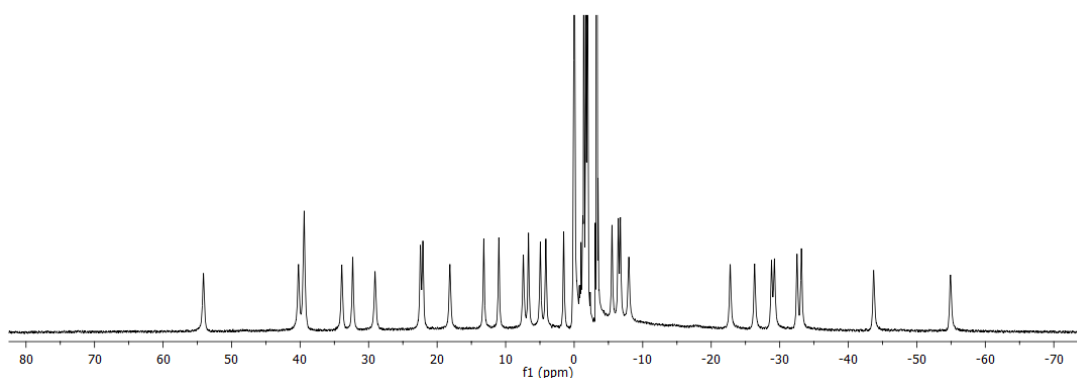
Figure S2 ^1H NMR spectra of the $[\text{Eu}(\text{do3aNN})]$ complex (~ 0.08 M solution in D_2O , $B_0 = 7.05$ T, $\text{pD} = 10.7$) at different temperatures. The chemical shift of HDO in the sample solution was referenced to 0 ppm.

Temperature dependence of ^1H NMR spectra of $[\text{Yb}(\text{do3aNN})]$ in D_2O

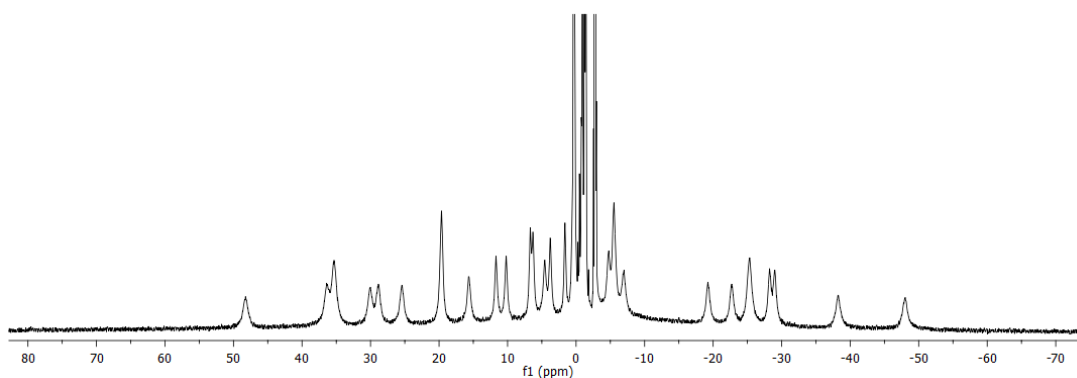
25 °C



50 °C



75 °C



90 °C

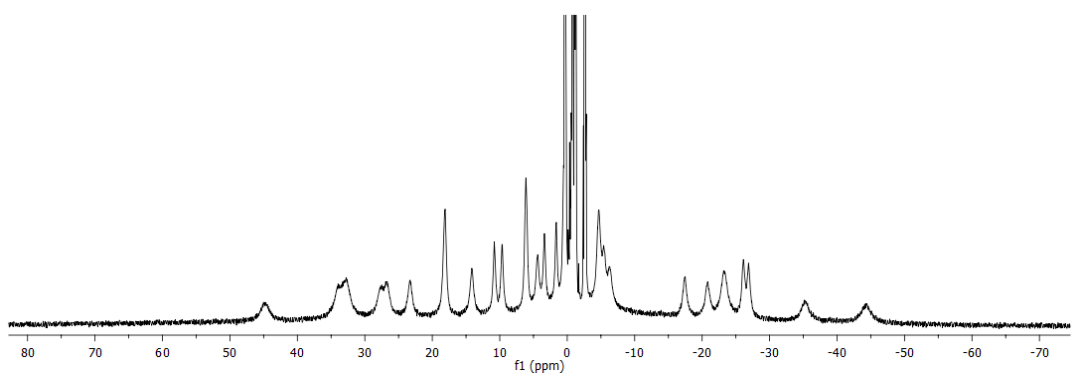
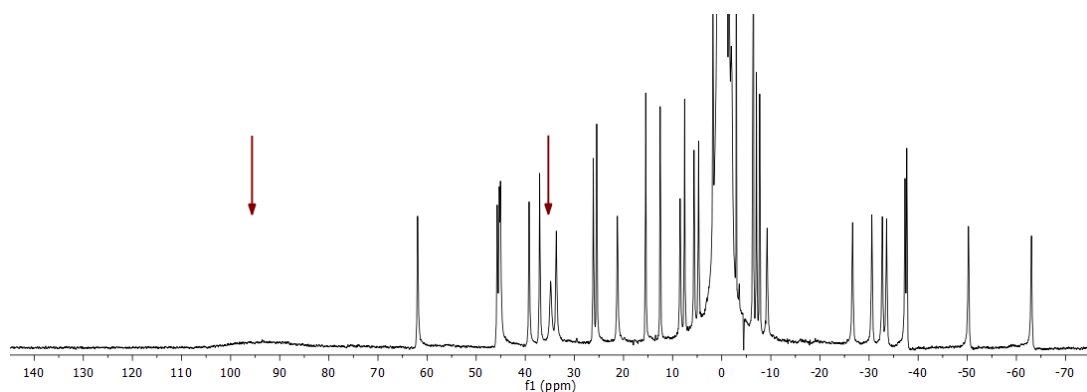


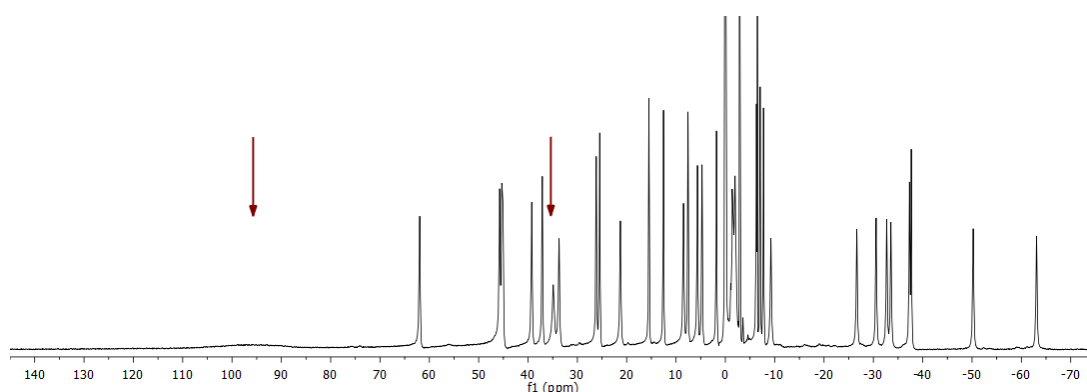
Figure S3 ^1H NMR spectra of the $[\text{Yb}(\text{do3aNN})]$ complex (~ 0.08 M solution in D_2O , $B_0 = 7.05$ T, $\text{pD} = 11.3$) at different temperatures. The chemical shift of HDO in the sample solution was referenced to 0 ppm.

pH dependence of ^1H NMR spectra of $[\text{Yb}(\text{do3aNN})]$

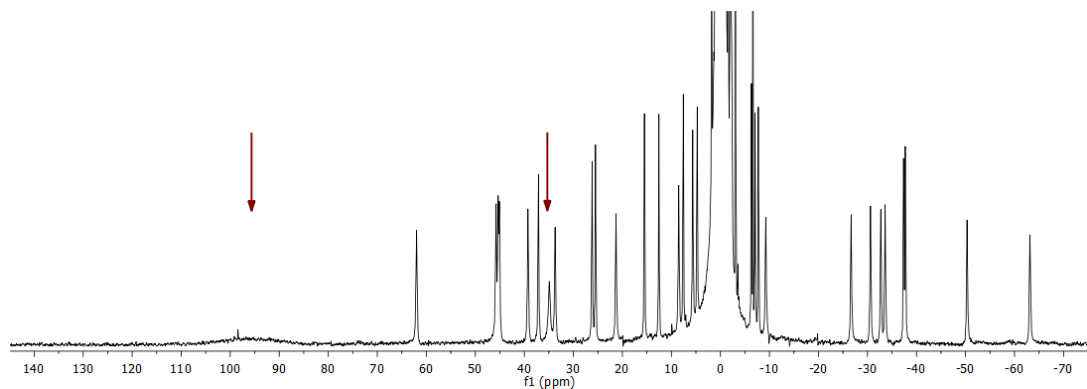
A



B



C



D

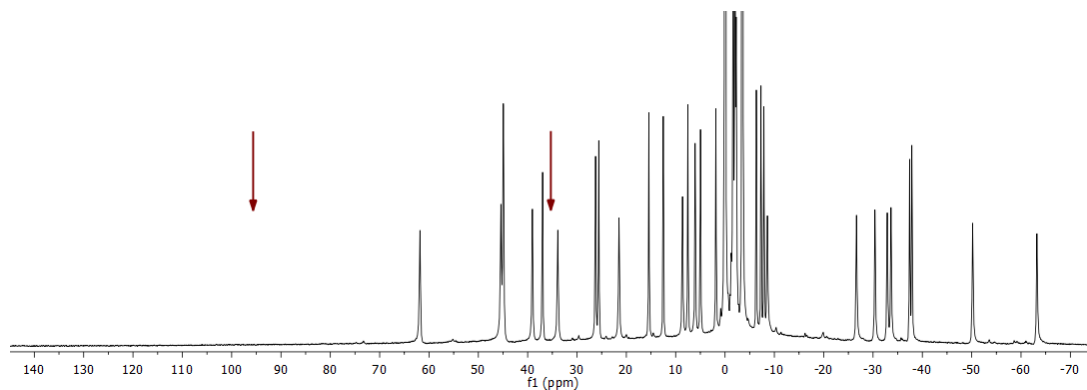
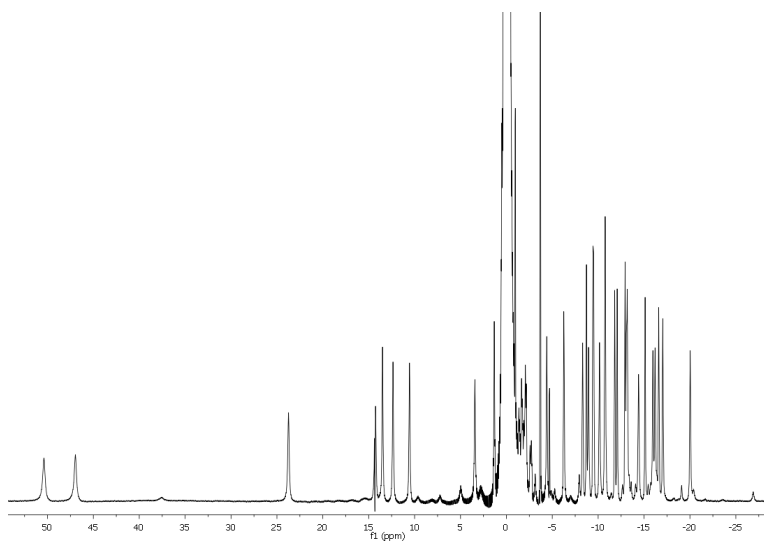


Figure S4 **A**: ^1H NMR spectrum of the $[\text{Yb}(\text{do3aNN})]$ complex, 0.09 M solution in H_2O , $B_0 = 7.05$ T, 25 $^\circ\text{C}$, pH = 9.38. **B**: the same sample, water signal was saturated. **C**: the same sample, pH was re-adjusted to 11.3. **D**: 0.04 M solution in D_2O , $B_0 = 7.05$ T, 25 $^\circ\text{C}$, pD = 11.34. Arrows show the positions of exchangeable (N-H) protons. The chemical shifts of $\text{H}_2\text{O}/\text{HDO}$ in the sample solutions were referenced to 0 ppm.

Low-temperature ^1H NMR spectra of $[\text{Eu}(\text{do3aNN})]$ and $[\text{Yb}(\text{do3aNN})]$ in H_2O

A



B

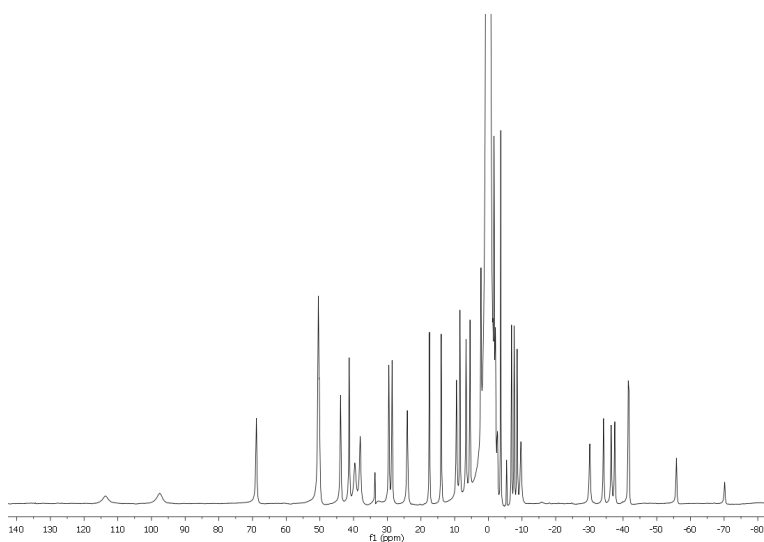
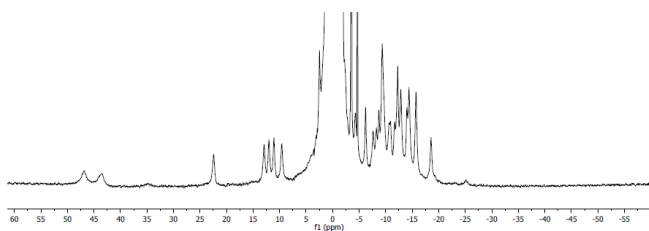


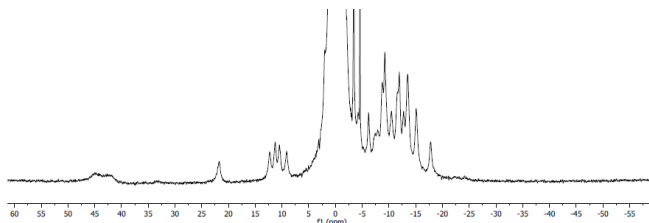
Figure S5 **A**: ^1H NMR spectrum of the $[\text{Eu}(\text{do3aNN})]$ complex, 47 mM solution in H_2O , $B_0 = 14.1$ T, 5°C , $\text{pH} = 9.5$. **B**: ^1H NMR spectrum of the $[\text{Yb}(\text{do3aNN})]$ complex, 45 mM solution in H_2O , $B_0 = 14.1$ T, 5°C , $\text{pH} = 9.6$. The chemical shifts of H_2O in the sample solutions were referenced to 0 ppm.

Temperature dependence of NMR spectra of [Eu(H₇do3aNN)] in H₂O

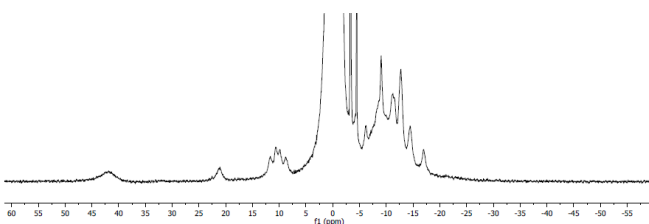
25 °C



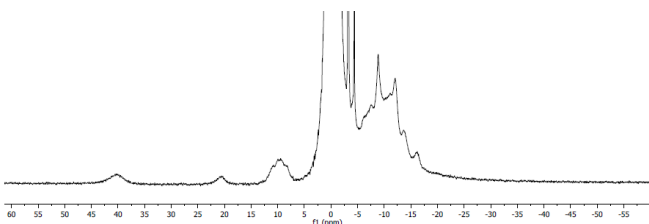
35 °C



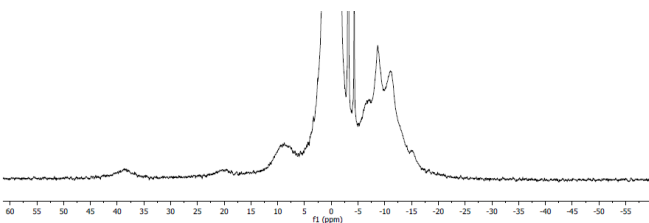
45 °C



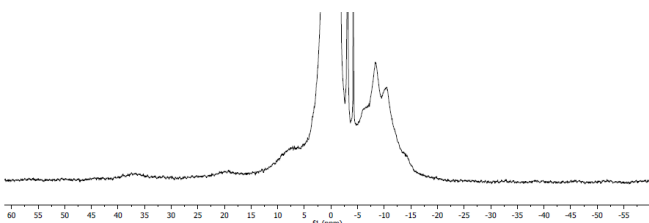
55 °C



65 °C



75 °C



85 °C

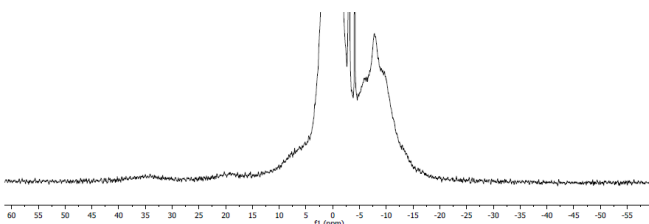
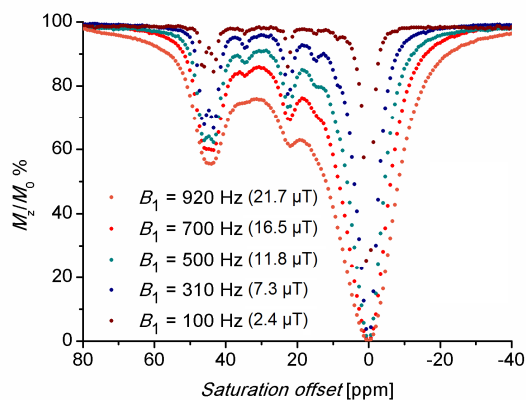


Figure S6 ¹H NMR spectra of the [Eu(H₇do3aNN)] complex (~0.05 M solution in H₂O, B₀ = 7.05 T, pH = 6.75) at different temperatures. The chemical shift of H₂O in the sample solution was referenced to 0 ppm.

Dependence of Z-spectra of $[\text{Eu}(\text{H}_n\text{do3aNN})]$ and $[\text{Yb}(\text{H}_n\text{do3aNN})]$ on presaturation intensity

A



B

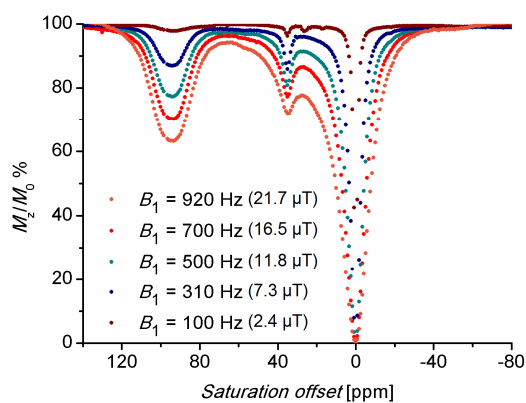


Figure S7 **A**: Z-spectra of an 87 mM aqueous solution of the $[\text{Eu}(\text{H}_n\text{do3aNN})]$ complex ($B_0 = 7.05$ T, RF presaturation pulse applied for 2 s, pH = 6.45, 25 $^\circ\text{C}$). **B**: Z-spectra of an 87 mM aqueous solution of the $[\text{Yb}(\text{H}_n\text{do3aNN})]$ complex ($B_0 = 7.05$ T, RF presaturation pulse applied for 2 s, pH = 6.33, 25 $^\circ\text{C}$).

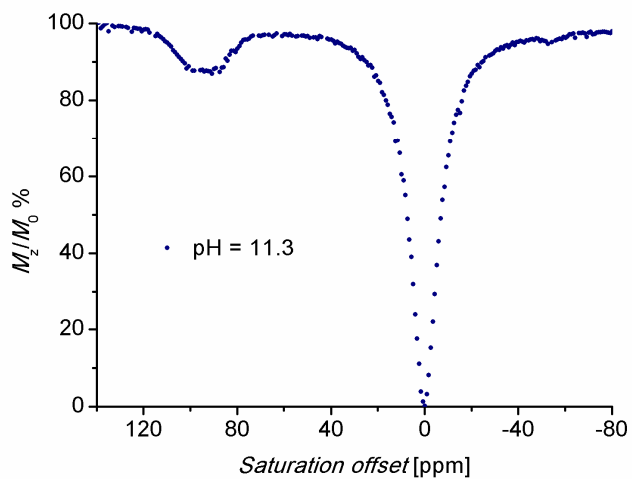
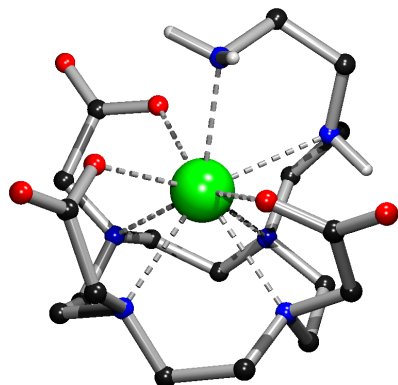


Figure S8 A: Z-spectra of an 87 mM aqueous solution of the [Yb(do3aNN)] complex at pH = 11.3 ($B_0 = 7.05$ T, $B_1 = 21.7$ μ T (920 Hz), RF presaturation pulse applied for 2 s, 25 $^{\circ}$ C).

Tentative visualization of TSA isomers differing in chirality of coordinated secondary amino group

A



B

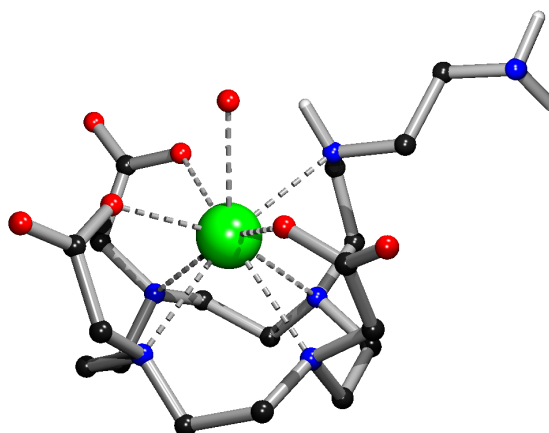
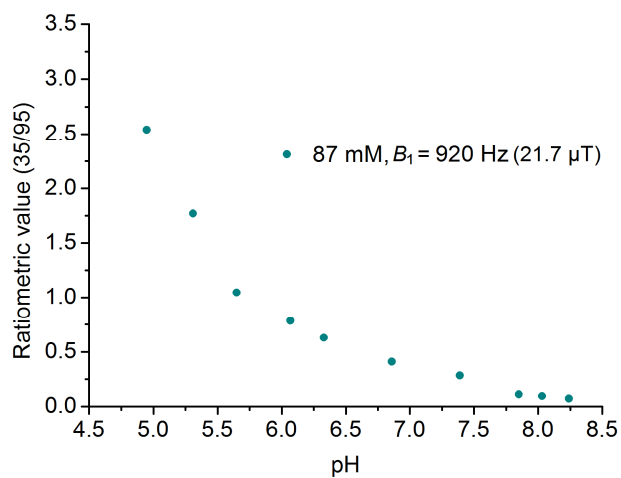


Figure S9 A: TSA $\Lambda\Lambda\Lambda\Lambda$ species with *R* chirality of the secondary amino group, enabling coordination of the primary amino group in the apical position. B: TSA $\Lambda\Lambda\Lambda\Lambda$ species with *S* chirality of the secondary amino group, disabling coordination of the primary amino group in the apical position. It should be noted that the primary amino group has to be fixed in position close to the central ion, as its protons have resolved the ^1H NMR signals and are still somewhat paramagnetically shifted. Such finding points to a some weak coordination of this group to the metal ion or its participation in an intramolecular hydrogen bond system.

Both structures were optimised with Gaussian package (Gaussian 09, Revision D.01)⁵ using DFT method with M06 functional⁶ and 6-31G(d,p) base set for all atoms but europium, where large core pseudopotential of Dolg et al. together with appropriate base set were used.⁷ Default value for integration grid (“fine”) and SCF convergence criteria 10e^{-8} were used. The stationary points found on the potential energy surfaces as a result of the geometry optimizations have been tested to represent energy minima *via* frequency analysis. Solvent effects were evaluated using the polarizable continuum model (PCM) as implemented in Gaussian.

pH dependence of MTR of $[\text{Eu}(\text{H}_n\text{do3aNN})]$ complex

A



B

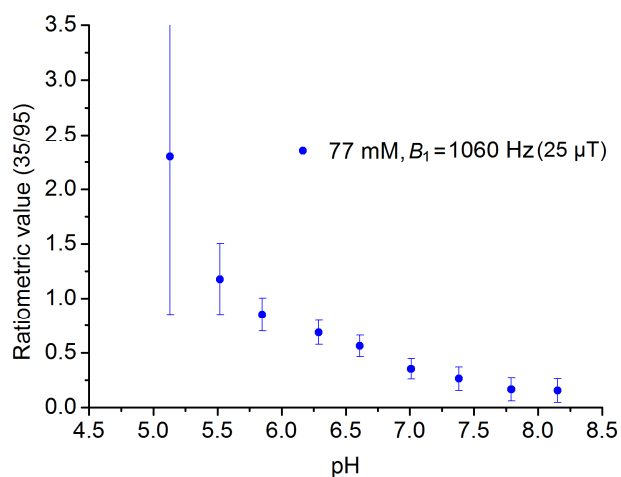


Figure S10 **A**: Ratiometric plot of an 87 mM aq. solution of the $[\text{Yb}(\text{H}_n\text{do3aNN})]$ complex at 25 °C taken by NMR; $B_0 = 7.05$, $B_1 = 21.7 \mu\text{T}$ (920 Hz), RF presaturation pulse applied for 2 s. **B**: Ratiometric plot of a 77 mM solution of the $[\text{Yb}(\text{H}_n\text{do3aNN})]$ complex in 50 mM HEPES–MES (1:1) at 25 °C taken by MRI; RARE pulse sequence, TR = 5 s, TE = 8.9 ms, $B_0 = 4.7$ T, $B_1 = 25 \mu\text{T}$ (1060 Hz), RF presaturation pulse applied for 2 s. The ratiometric value (35/95) is the ratio of the MTR intensity at 35 ppm to the MTR intensity at 95 ppm.

^1H and $^{13}\text{C}\{^1\text{H}\}$ NMR spectra of $\text{H}_3\text{do3aNN}$

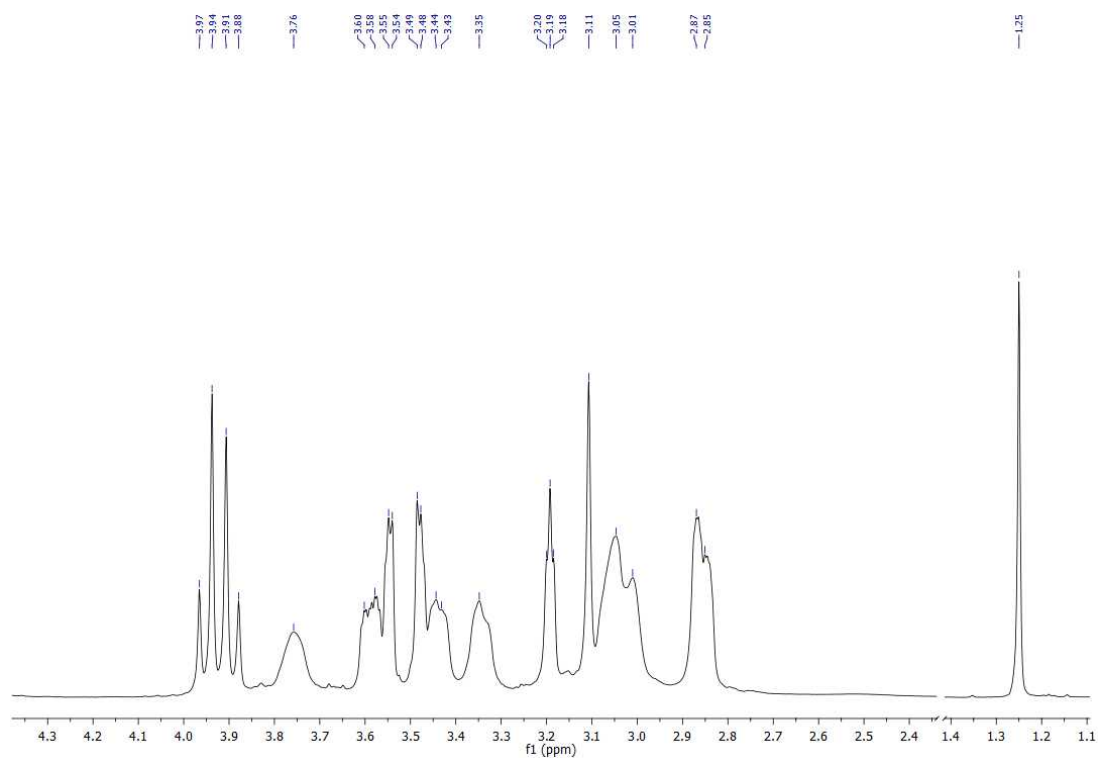


Figure S11 ^1H NMR spectrum of $\text{H}_3\text{do3aNN}$ in D_2O , pD = 6.07, 55 °C.

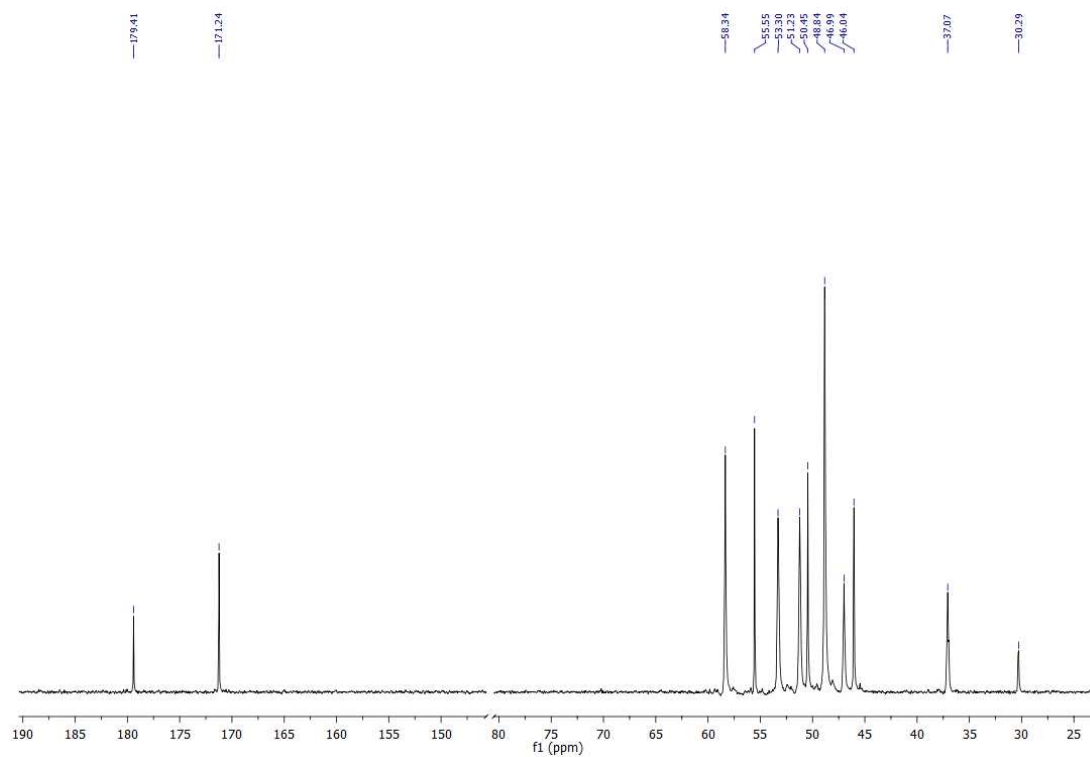


Figure S12 $^{13}\text{C}\{^1\text{H}\}$ NMR spectrum of $\text{H}_3\text{do3aNN}$ in D_2O , pD = 6.07, 55 °C.

Potentiometric studies – protonation and stability constants of H₃do3aNN and its Eu(III)/Yb(III) complexes

Table S1 Overall protonation constants ($\log b_h$)^[a] of H₃do3aNN (0.1 M NMe₄Cl, 25 °C).

h	$\log b_h$
1	12.62(2)
2	22.90(2)
3	32.57(2)
4	40.87(3)
5	44.17(3)
6	45.75(3)

^[a] $b_h = [\text{H}_h\text{L}]/\{[\text{H}]^h \cdot [\text{L}]\}$

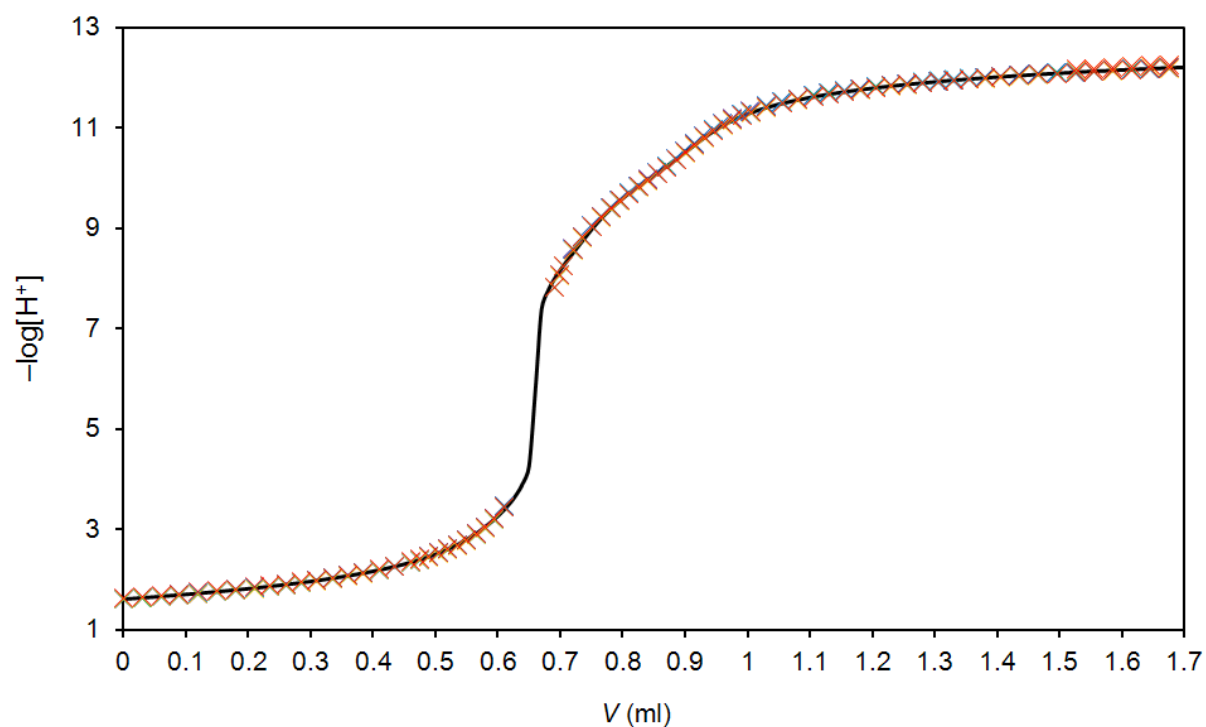


Figure S13 Titration data of the acid-base titration of the free ligand H₃do3aNN showing the best fit calculated using the protonation constants from Table S1 ($c_L = 0.004$ M, 0.1 M NMe₄Cl, 25 °C).

Table S2 Overall stability constants ($\log b_{hlm}$)^[a] of $[\text{Ln}(\text{H}_n\text{do3aNN})]$ complexes (0.1 M NMe_4Cl , 25 °C).

$\log b_{hlm}$				
<i>h</i>	<i>l</i>	<i>m</i>	Eu	Yb
0	1	1	23.16(5)	22.76(4)
1	1	1	29.19(4)	28.98(3)
2	1	1	34.28(7)	34.05(4)

^[a] $b_{hlm} = [\text{H}_h\text{L}_l\text{M}_m] / \{[\text{H}]^h \cdot [\text{L}]^l \cdot [\text{M}]^m\}$

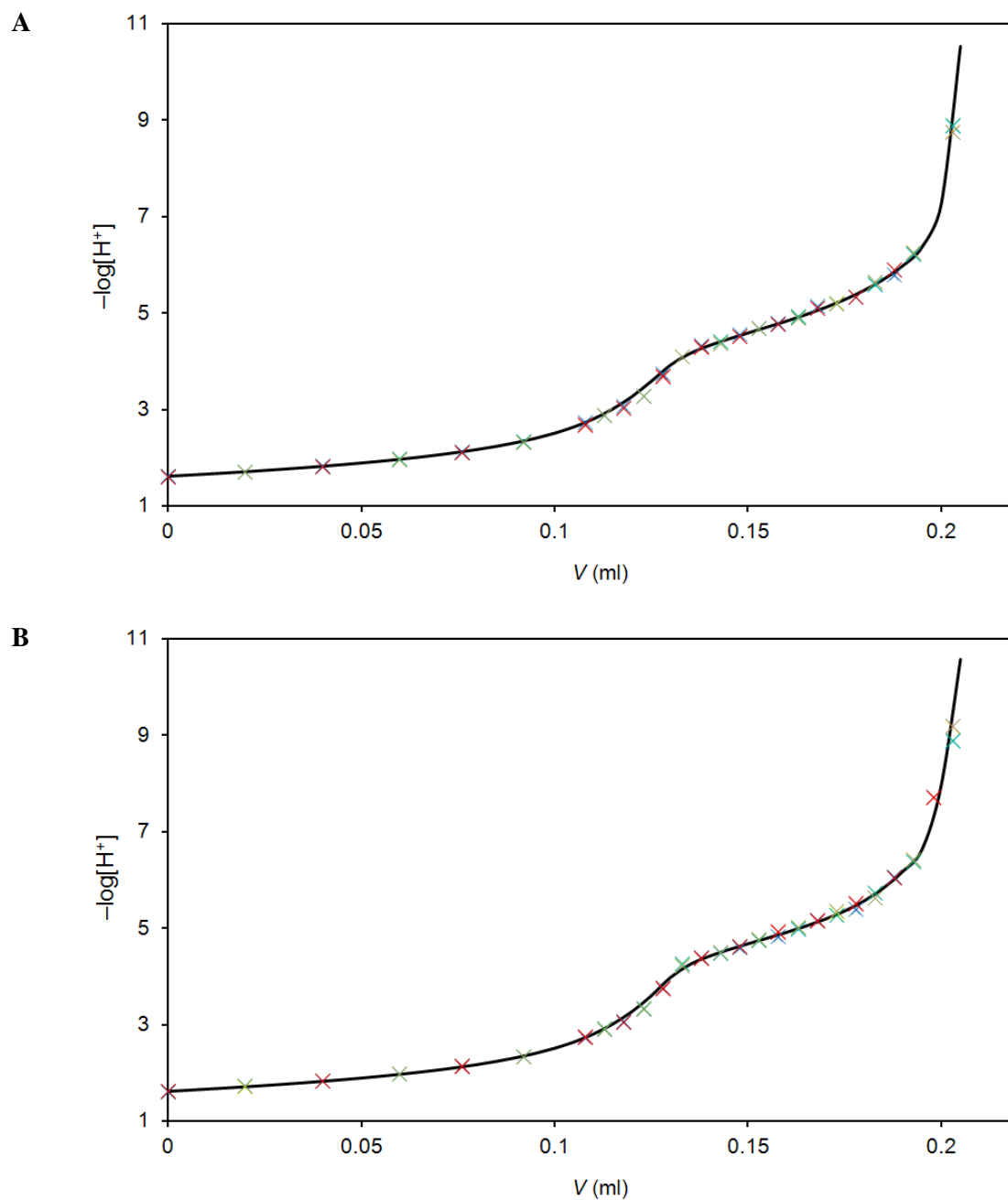


Figure S14 Titration data of the out-of-cell titration of $\text{Ln}(\text{III})\text{-H}_3\text{do3aNN}$ systems showing the best fits calculated using the stability constants from Table S2 ($c_M = c_L = 0.004$ M, 0.1 M NMe_4Cl , 25 °C, equilibration time = 7 weeks). **A:** $\text{Eu}(\text{III})\text{-H}_3\text{do3aNN}$ system. **B:** $\text{Yb}(\text{III})\text{-H}_3\text{do3aNN}$ system.

Table S3 Overall protonation constants ($\log b_{h11}$)^[a] of [Ln(do3aNN)] complexes (0.1 M NMe₄Cl, 25 °C).

h	$\log b_{h1\text{Eu}}$	$\log b_{h1\text{Yb}}$
1	5.57(3)	5.67(1)
2	10.41(2)	10.52(1)

^[a] $b_{h11} = [\text{H}_h\text{LM}]/\{[\text{H}]^h \cdot [\text{LM}]\}$

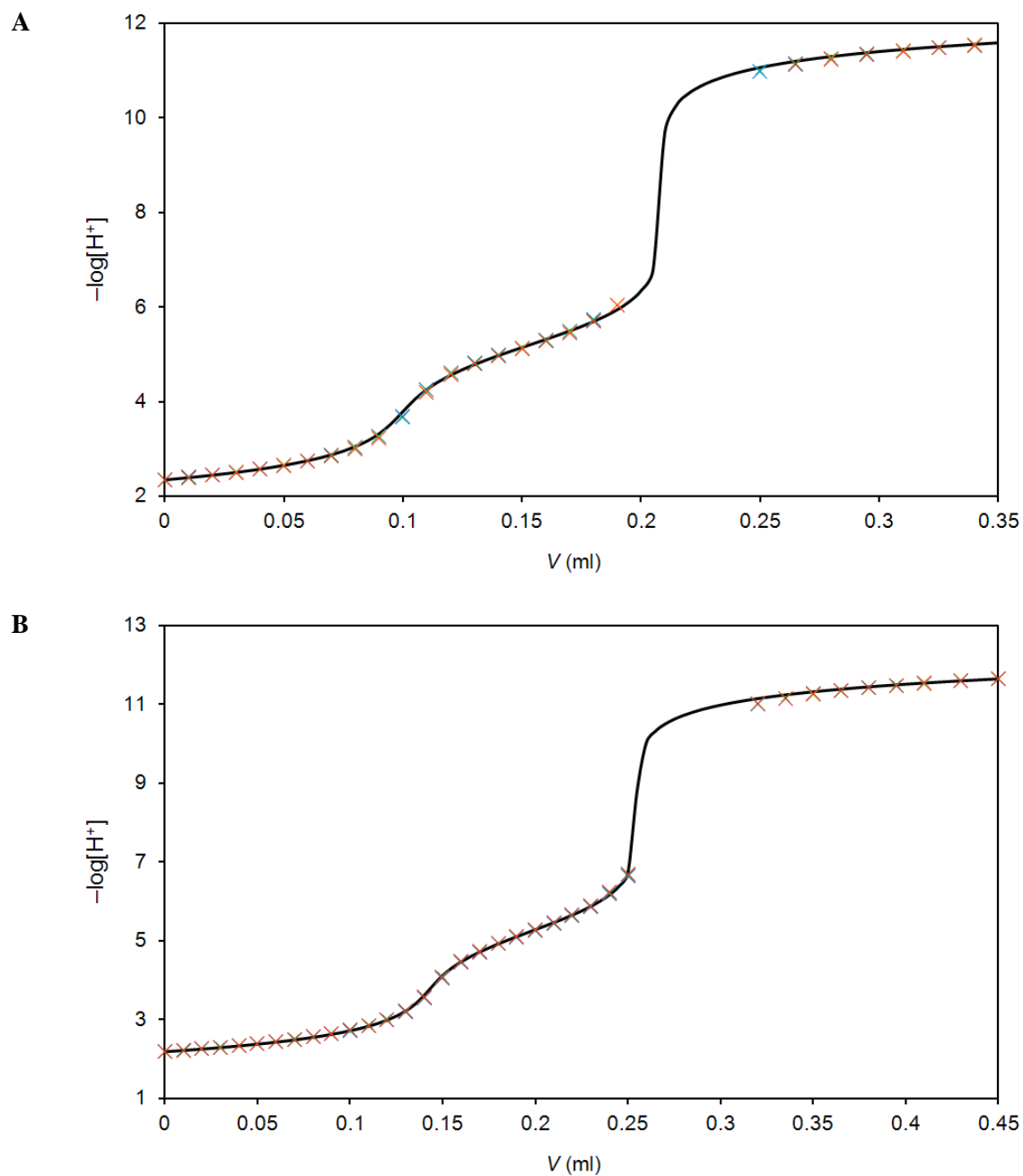
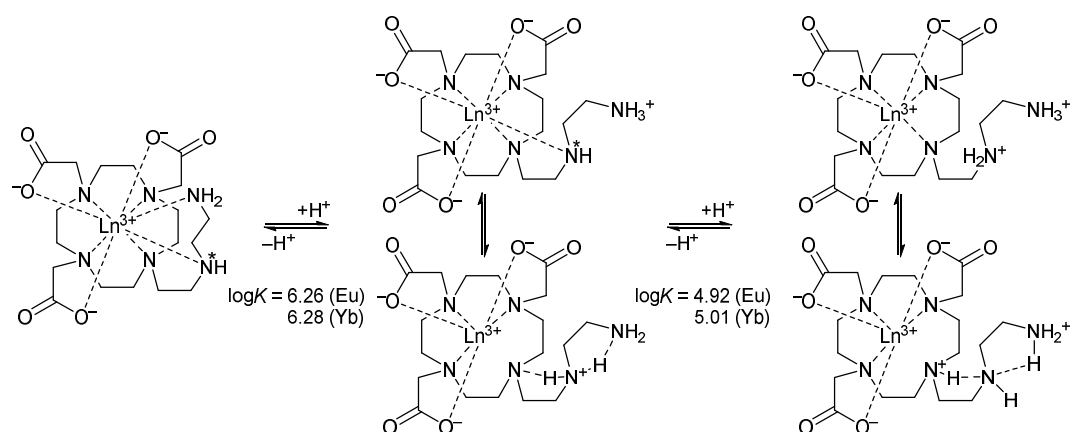
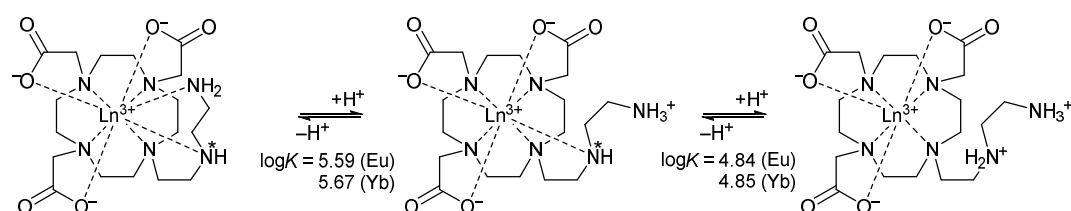


Figure S15 Titration data of the acid-base titration of the pre-formed [Ln(do3aNN)] complexes with the best fits calculated using the protonation constants from Table S3 ($c_{\text{ML}} = 0.003$ M, 0.1 M NMe₄Cl, 25 °C). **A:** H⁺-[Eu(do3aNN)] system. **B:** H⁺-[Yb(do3aNN)] system.

Schemes – suggested protonation sites of complex species



Scheme S1 Suggested species with the tentative protonation sites present in the protonation equilibrium of Ln(III)–H₃do3aNN mixtures during out-of-cell titration. In the protonated species, binding of the water molecule(s) to the central ion filling its coordination sphere to the coordination number 8–9 is expected, but it is not shown for the sake of clarity



Scheme S2 Suggested species occurring during the non-equilibrium potentiometric acid-base titration of pre-formed [Ln(do3aNN)] complexes. In the hepta/octa-coordinated species, binding of the water molecule(s) to the central ion filling its coordination sphere to the coordination number 8–9 is expected, but it is not shown for the sake of clarity.

UV-Vis spectrophotometry

UV-Vis solution spectra were obtained on a SPECORD® 50 PLUS (ANALYTIC JENA AG) spectrophotometer at 25 °C in the range of 300–1000 nm with the data intervals of 0.2 nm and the integration time of 0.04 s.

The samples for UV-Vis spectra of xylenol orange–Eu³⁺ complex were prepared by the following way: 100 µl of xylenol orange solution (10⁻⁴ M) in buffer (mixture of 0.025 M aq. HEPES and 0.025 M aq. MES; pH = 5.55) was added to 898 µl of the same buffer (pH = 5.55). Gradually, 2.2 µl portions of aq. solution of EuCl₃ in H₂O (4.46 mM) were added, and the UV-Vis spectrum was acquired after each addition (Figure S16).

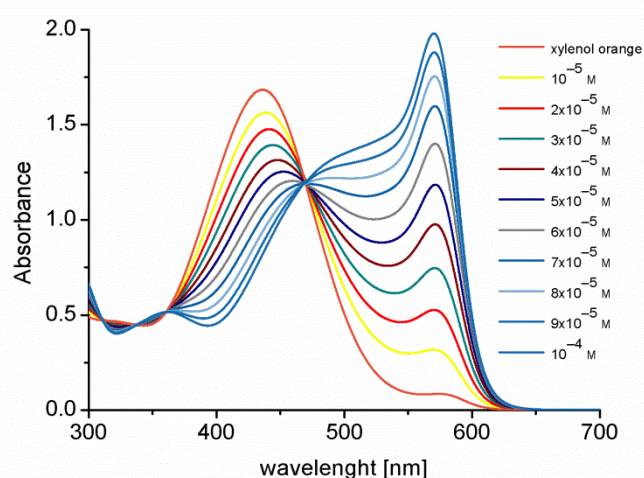


Figure S16 Change of UV-Vis spectra of aq. solution of xylenol orange (10⁻⁵ M, pH = 5.55, 0.025 M HEPES and 0.025 M MES, 25 °C) with increasing concentration of EuCl₃ (10⁻⁵–10⁻⁴ M).

Kinetic stability of [Eu(H_ndo3aNN)] complex was studied by following procedure: 100 µl of aq. solution of [Eu(do3aNN)] complex (8 mM, pH = 7.5) was added to the mixture of 800 µl of buffer solution (mixture of 0.025 M aq. HEPES and 0.025 M aq. MES, pH = 5.55) with 100 µl of xylenol orange solution (10⁻⁴ M) in the same buffer (pH = 5.55). The evaluation of the absorption spectra with time was measured and is shown in Figure S17.

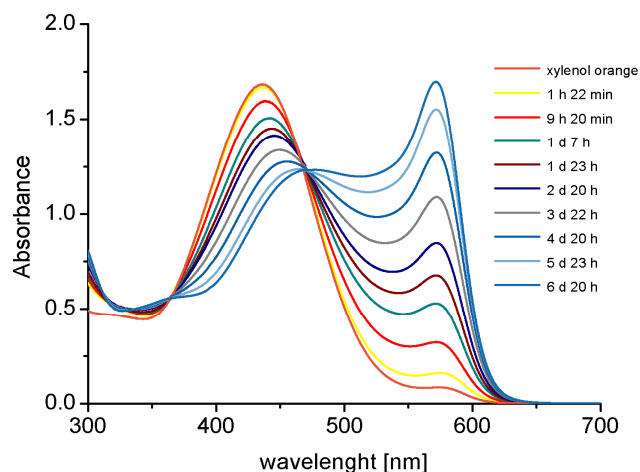


Figure S17 Time dependence of UV-Vis spectra of aq. solution of xylenol orange (10^{-5} M, pH = 5.55, 0.025 M HEPES and 0.025 M MES, 25 °C) in the presence of the $[\text{Eu}(\text{H}_n\text{do3aNN})]$ complex ($8 \cdot 10^{-4}$ M).

References

-
- ¹ G. M. Sheldrick, SHELXS97, Program for Crystal Structure Solution from Diffraction Data, University of Göttingen, Göttingen, 1997.
 - ² G. M. Sheldrick, SHELXL97, Program for Crystal Structure Refinement from Diffraction Data, University of Göttingen, Göttingen, 1997.
 - ³ T. Krchová, J. Kotek, D. Jiráček, J. Havlíčková, I. Císařová and P. Hermann, *Dalton Trans.*, 2013, **42**, 15735–15747.
 - ⁴ M. Meyer, V. Dahaoui-Gindrey, C. Lecomte and R. Guilard, *Coord. Chem. Rev.*, 1998, **178–180**, 1313–1405.
 - ⁵ M. J. Frisch, G. W. Trucks, H. B. Schlegel, G. E. Scuseria, M. A. Robb, J. R. Cheeseman, G. Scalmani, V. Barone, B. Mennucci, G. A. Petersson and et al., Gaussian 09, Revision D.01, Gaussian, Inc.: Wallingford.
 - ⁶ Y. Zhao and D. G. Truhlar, *Theor. Chem. Acc.*, 2008, **120**, 215–241.
 - ⁷ M. Dolg, H. Stoll and H. Preuss, *Theor. Chim. Acta*, 1993, **85**, 441–450.